MCB
Journals.ASM.org

$P2Y_4$ Receptor-Mediated Pinocytosis Contributes to Amyloid Beta-Induced Self-Uptake by Microglia

Hui-quan Li,[a,b] Cong Chen,[b] Ying Dou,[a] Hang-jun Wu,[b] Yi-jun Liu,[b] Hui-Fang Lou,[b] Jian-min Zhang,[c] Xiao-ming Li,[b] Hao Wang,[b] Shumin Duan[a,b]

Institute of Neuroscience and Key Laboratory of Neuroscience, Shanghai Institutes for Biological Sciences, Chinese Academy of Sciences, Shanghai, China[a]; Department of Neurobiology, Key Laboratory of Medical Neurobiology of the Ministry of Health of China, Key Laboratory of Neurobiology of Zhejiang Province, Zhejiang University School of Medicine, Hangzhou, China[b]; Department of Neurosurgery, Second Affiliated Hospital, Zhejiang University School of Medicine, Hangzhou, China[c]

Brain disturbances, like injuries or aberrant protein deposits, evoke nucleotide release or leakage from cells, leading to microglial chemotaxis and ingestion. Recent studies have identified $P2Y_{12}$ purinergic receptors as triggers for microglial chemotaxis and $P2Y_6$ receptors as mediators for phagocytosis. However, pinocytosis, known as the internalization of fluid-phase materials, has received much less attention. We found that ATP efficiently triggered pinocytosis in microglia. Pharmacological analysis and knockdown experiments demonstrated the involvement of $P2Y_4$ receptors and the phosphatidylinositol 3-kinase/Akt cascade in the nucleotide-induced pinocytosis. Further evidence indicated that soluble amyloid beta peptide 1-42 induced self-uptake in microglia through pinocytosis, a process involving activation of $P2Y_4$ receptors by autocrine ATP signaling. Our results demonstrate a previously unknown function of ATP as a "drink me" signal for microglia and $P2Y_4$ receptors as a potential therapeutic target for the treatment of Alzheimer's disease.

Microglia are the resident phagocytes in the central nervous system (CNS) and are responsible for the maintenance of CNS homeostasis (1, 2). They take up invasive microorganisms, apoptotic/necrotic cellular debris, and the aberrant protein depositions in progressive neurodegenerative disorders, including the amyloid beta (Aβ) peptides in Alzheimer's disease (AD) (3). Understanding the mechanisms of endocytosis in these cells is thus relevant to understanding their functions.

Phagocytosis and pinocytosis are two clathrin-independent endocytic processes that occur in phagocytes, and both create large endocytic vacuolar compartments (>0.2 μm) through organized membrane movements and actin polymerization (4). Nevertheless, distinct models and molecular mechanisms have been suggested for the formation of phagosomes and pinosomes (4). The well-studied Fc receptor-mediated phagocytosis is guided by a zipper-like progression of receptor-initiated membrane invagination that is shaped by the geometry of the internalized particle, whereas pinosomes, which may vary from 0.2 to 10 μm in diameter, are suggested to form spontaneously or in response to growth factor receptor stimulation from membrane ruffles that close at their distal margins to engulf extracellular fluid without strict guidance from receptors (4, 5). Phagocytosis in phagocytes is known to be triggered by "eat me" signals expressed on the cell surface of dying cells (6). In addition, UDP leakage from damaged neurons has been suggested to function as a diffusible "eat me" signal to induce phagocytic activity in microglia through activation of $P2Y_6$ receptors (7). Pinocytosis by phagocytes is involved in many physiological and pathological processes, including development, innate immunity, and the entry of pathogens into host cells (4, 5). However, the mechanisms underlying the regulation of pinocytosis in microglia are not clear. In the present study, we found that ATP triggered microglial pinocytosis through activation of $P2Y_4$ purinergic receptors. The phosphatidylinositol 3-kinase (PI3K)/Akt cascade was shown to be the downstream pathway of the ATP-induced pinocytosis. Interestingly, soluble Aβ itself induced pinocytosis, which is an ATP/$P2Y_4$-dependent process, indicating that microglial pinocytosis of Aβ is a nucleotide-regulated active process, rather than a constitutive, passive activity. Moreover, either $P2Y_4$ knockdown by RNA interference or ATP deprivation by the ATP-degradation enzyme apyrase decreased the spontaneous pinocytosis of Aβ by microglia. Thus, in addition to the previously identified $P2Y_{12}$ receptor-mediated "find me" signal (8–10) and the $P2Y_6$ receptor-mediated "eat me" signal (7), our study demonstrates that nucleotides also function as an autocrine "drink me" signal for microglia and mediate the uptake of soluble Aβ through activation of $P2Y_4$ receptors.

MATERIALS AND METHODS

Animals. The use and care of animals followed the guidelines of the Shanghai Institutes for Biological Sciences Animal Research Advisory Committee (Shanghai, China) and the Animal Advisory Committee at Zhejiang University, which approved the protocols. APPswe/PS1dE9 transgenic mice on a C3H background were obtained from the Jackson Laboratory (Bar Harbor, ME).

Cell culture. Primary cultured microglia were harvested according to a method described previously (11). In brief, a mixed glial culture was prepared from the cortices of neonatal Sprague-Dawley rats (either sex) and maintained for 7 to 10 days in minimum essential medium (MEM; Gibco, Grand Island, NY) containing 10% fetal bovine serum (FBS; Gibco). The cells floating over the mixed glial culture were collected by gentle shaking and transferred to appropriate glass coverslips. Microglia

Received 7 May 2013 Returned for modification 13 June 2013
Accepted 23 August 2013
Published ahead of print 3 September 2013
Address correspondence to Shumin Duan, duanshumin@zju.edu.cn.
H.-Q.L. and C.C. contributed equally to this work.
Supplemental material for this article may be found at http://dx.doi.org/10.1128/MCB.00544-13.

doi:10.1128/MCB.00544-13

were obtained as rapidly attached cells and maintained in low-FBS medium (2% FBS in MEM) for 12 to 24 h before use.

Mixed glial cultures can also give rise to purified secondary astrocytes. As previously described (12), mixed glial cultures were shaken at 200 rpm overnight at 37°C to dislodge other glial cells attached to the astrocyte layer. After medium replacement, astrocytes were obtained by trypsinization (0.125% trypsin, 5 min, 37°C) and replated at a low density. When the cell density reached 70%, they were used for drug treatment or transfection experiments.

Primary pure neuronal cultures were prepared as described previously (13) with some modifications. In brief, embryonic day 18 (E18) rat (either sex) hippocampi were dissected, dissociated with 0.125% trypsin, and plated on coverslips coated with Matrigel (Sigma-Aldrich, St. Louis, MO) at a cell density of 60,000/ml in neurobasal medium (Gibco) supplemented with 2% B27 (Sigma-Aldrich) and 0.25% glutamine (Sigma-Aldrich). Thereafter, half of the medium was replaced twice a week with neurobasal medium containing 2% B27 supplement and 0.25% glutamine. Neurons were used 6 to 8 days after plating.

Pinocytosis and phagocytosis assay. Fluorophore-linked dextrans used to label pinosomes were all obtained from Invitrogen (Carlsbad, CA). Nonfixable FD70S (fluorescein-labeled dextrans with an average molecular weight of 70,000) and TD3S (Texas Red-labeled dextrans with an average molecular weight of 3,000) were used to measure fluid-phase pinocytosis in live cells, while for combined immunostaining, lysine-fixable TD70S (lysine-fixable Texas Red-labeled dextrans with an average molecular weight of 70,000) was used to label pinosomes. Fluorescent-labeled latex beads (red; 0.5 μm in diameter) were obtained from Sigma-Aldrich. Generally, cells were incubated in MEM with fluorescent probes and agonists for 5 min, thoroughly washed with Hanks balanced salt solution, and then either placed under a confocal microscope for observation or fixed for immunostaining. The agonists adenosine 5′-*O*-(3-thio) triphosphate (ATPγS), UTP, and ATP were all obtained from Sigma-Aldrich. Aβ1-42, used as an agonist in some experiments, was from AnaSpec, Inc. (San Jose, CA).

Preparation of soluble Aβ1-42 and detection of Aβ internalization. 6-Carboxyfluorescein (FAM)-labeled Aβ1-42 and Texas Red-labeled Aβ1-42 were used to detect internalized Aβ peptides. All of the Aβ peptides were obtained from Anaspec (San Jose, CA). For soluble Aβ preparation, lyophilized Aβ peptide was dissolved completely in 0.1% NH_4OH to 2 mM and stored at −80°C until use. Before use, Aβ stock solution was swiftly dissolved into a working solution (usually dissolved in minimum essential medium). This working solution was verified as fibril-free via sodium dodecyl sulfate-polyacrylamide gel electrophoresis (SDS-PAGE). Only those solutions without any Aβ aggregates bigger than 10 kDa were used for further experiments.

Migration assay. The migration assay was performed according to a method described previously (11). Purified microglia growing on coverslips were transferred to chambers filled with 1 ml of L-15 medium (Gibco). The chambers were then sealed with silicone oil and placed on a temperature-controlled stage heater set at 37°C above a microscope (Olympus IX50; Japan) connected to a camera (JVC TK-C1381; Japan). Gradients of chemicals were produced by methods described previously (14). Repetitive pressure injection of picoliter volumes of solutions containing ATPγS was applied through a micropipette with a tip opening of ~2 μm. The pressure was applied with an electrically gated pressure application system (Picosprizer II; Parker Co.). A standard pressure pulse of 3 lb/in^2 in amplitude and 20 ms in duration was applied to the pipette at a frequency of 2 Hz by using a pulse generator (Nihon Kohden, Japan). Local perfusion of drugs was performed using glass micropipettes positioned 50 to 70 μm from the target cell. Previous studies had shown that the concentration of a drug 100 μm from the pipette tip is $\sim 10^3$-fold lower than that in the pipette under standard conditions (14). For cell mask experiments, microglia were pretreated with cell mask fluorescent dyes (1 μg/ml; Invitrogen) for 3 min on ice, and then the chambers were placed on a temperature-controlled stage heater set at 37°C above the confocal microscope with a 60×/1.2 numerical aperture (NA), water immersion, differential interference contrast (DIC) objective lens. Fluoview software was used to collect images.

Drug treatments. The effects of the inhibitors amiloride, RB2, suramin, MRS2395, and MRS2578 (all from Sigma-Aldrich) and also wortmannin and LY294002 (both from Fermentek, Jerusalem, Israel) were assessed after a 30-min preincubation at the indicated concentrations, followed by incubation with endocytic probes and agonists, with the relevant inhibitors still present. The effect of apyrase (Sigma-Aldrich) was assessed after a 6-h preincubation. Control cells were treated with 1% L-15 medium or 0.1% dimethyl sulfoxide (the final concentrations in the antagonist vehicle).

Cell transfection and knockdown efficiency examination. For the knockdown experiments, double strands of small interfering RNA (siRNA) oligonucleotides end-capped with FAM fluorescent linkages were designed according to the primary sequence of each P2Y receptor. All of the siRNA oligonucleotides were obtained from Invitrogen and transfected with Oligofectamine (Invitrogen) according to the manufacturer's instructions.

$P2Y_4$ siRNA pools (a mixture of three oligonucleotide duplexes) were as follows: duplex 1, 5′-AACTGCATAGCTCATAGGC (antisense); duplex 2, 5′-AATTGTGCGGGTGATGTGG (antisense); duplex 3, 5′-TTG AACTCCTCATTAAACC (antisense). In addition, we used the $P2Y_6$ siRNA sequence, 5′-TGCCATTGTCCCGCTCCAT (antisense), and $P2Y_2$ siRNA sequence, 5′-ACGCCATCAACATGGCGTATT (antisense). Stealth Block-iT siRNA (Invitrogen) was used as the control.

The transfection efficiency in primary microglia cultures was very low (less than 20% of cells could be transfected). Since the mechanism of RNA interference is highly conserved (15, 16), we examined the knockdown efficiency of siRNAs in rat primary astrocyte cultures, which also express various subtypes of P2Y receptors and have transfection efficiencies higher than 80%.

The knockdown efficiency of RNA was examined by reverse transcription-PCR (RT-PCR), except for the $P2Y_4$ receptor siRNA, which was examined for both the protein level, by Western blotting, and RNA level, by RT-PCR. Total RNA extracts from astrocytes were harvested 72 h after siRNA transfection. Briefly, total RNA was isolated by using TRIzol (Invitrogen) and purified with phenol-chloroform (Sangon Biotech, China) according to the manufacturer's instructions. RT was performed with 1 μg of total RNA by using the PrimeScript RT reagent kit with a genomic DNA (gDNA) Eraser (TaKaRa, Japan). One microliter of the RT product was added to the reaction mixture containing 2× PCR master mix (Shanghai Lifefeng Biotech, China), and P2Y receptor-specific primers, including the following: for $P2Y_2$ (543 bp), forward (F), 5′-GGTTTATT ACTACGCCCAGG-3′, and reverse (R), 5′-AAGGAGTAATAGAGGGT GCG-3′; for $P2Y_4$ (454 bp), F, 5′-TGGGTGTTTGGTTGGTAGTA-3′, and R, 5′-GTCCCCCGTGAAGAGATAG-3′; for $P2Y_6$ (516 bp), F, 5′-GT GGTATGTGGAGTCGTTTG-3′, and R, 5′-CTGTAGGAGATCGTGTG GTT-3′. After PCR amplification, the products were detected by agarose gel electrophoresis on a 10% agarose gel, which was stained with GoldView (SBS Genetech, Shanghai, China) and photographed.

Immunostaining. Microglia plated on coverslips were fixed with 4% paraformaldehyde in phosphate-buffered saline (PBS) at 4°C for 10 min, permeabilized with pure methanol at −20°C for 20 min, and treated with 5% FBS for 1 h at 25°C. Cultures were then stained with one or two of the following antibodies overnight at 4°C: rabbit anti-$P2Y_2$ (1:200; Abcam), rabbit anti-$P2Y_4$ (1:200; Abcam), mouse anti-Akt (1:70; Cell Signaling), and rabbit anti-phosphorylated Akt (1:70; Cell Signaling). After washing with PBS to remove excess primary antibodies, the cultures were incubated for 1 h at room temperature with the fluorescence-conjugated secondary antibodies anti-mouse IgG–Cy3 and anti-rabbit IgG–Alexa Fluor 488 (Jackson ImmunoResearch, West Grove, PA). Excess antibody was removed by washing cultures 4 times, and cells were imaged with the confocal microscope.

Coronal sections (30 μm) of the cortex from male mice were incu-

bated for 2 h at room temperature in a blocking solution (10% bovine serum) and then incubated for 48 h at 4°C with the primary antibodies. Anti-Iba1 (1:300; Abcam) was used as a microglial marker. Antibody to the $P2Y_4$ receptor (1:200) was from Acris (Herford, Germany). Following incubation, sections were washed and incubated for 2 h at 37°C with the secondary antibody (anti-rabbit IgG-conjugated Alexa Fluor 488 or anti-goat IgG-conjugated Alexa Fluor 546; 1:1,000; Molecular Probes, Carlsbad, CA).

Image analysis. Live imaging was carried out on the Olympus confocal microscope with a 60×/NA 1.2 water objective and 488/543-nm laser lines. Cells were incubated in chambers placed on a temperature-controlled stage heater set at 37°C. The Fluoview software was used to collect images. For immunostained samples, an A1 confocal microscope (Nikon, Japan) equipped with a 60×/NA 1.4 oil objective and 488/543-nm laser lines was used, and NIS Elements software was used to collect images. Images were taken at room temperature. Stacks of sections were obtained over a cell thickness of 5 μm at a spacing of every 125 nm. Raw images were processed and reconstructed in three dimensions by using the LSM5 image browser software (Carl Zeiss). Image analysis was performed with Image Pro Plus 5.1 (Media Cybernetics, Bethesda, MD), ImageJ (National Institutes of Health), NIS Elements imaging software (Nikon, Japan), or AutoQuant X2 (Media Cybernetics).

Western blotting. For knockdown experiments, protein extracts from astrocytes were harvested 72 h after siRNA transfection and separated on 12% polyacrylamide gels, followed by transfer to polyvinylidene difluoride membranes by wet blotting. We performed protein detection according to the standard method of enhanced chemiluminescence Western blotting (Amersham Pharmacia Biotech). The rabbit anti-$P2Y_4$ antibodies (Abcam) were added at a dilution of 1:2,000, while the mouse anti-glyceraldehyde 3-phosphate dehydrogenase (anti-GAPDH) antibodies (Kangchen Biotech, Shanghai, China) were added at 1:10,000.

For the verification of $P2Y_4$ expression, protein extracts from primary cultured microglia were harvested and detected with anti-$P2Y_4$ antibodies (Abcam) at a dilution of 1:2,000.

For Akt phosphorylation experiments, protein extracts from primary cultured microglia were detected with rabbit anti-phosphorylated Akt antibodies (Cell Signaling) at a dilution of 1:5,000 and mouse anti-Akt antibodies (Cell Signaling) at 1:5,000. The mouse anti-GAPDH antibodies (Kangchen Biotech) were added at 1:10,000.

Extracellular ATP measurements. The concentration of extracellular ATP was quantified via a bioluminescence method that employed the luciferase-luciferin test. In brief, the culture medium of microglia was replaced with a recording medium containing a mixture of ectonucleotidase inhibitors. The inhibitors, including dipyridamole (100 μM), AMP-CP (50 μM), and ARL67165 (50 μM), were added into the extracellular solution throughout the experiment to decrease ATP degradation. Aβ1-42, Aβ1-40, or Aβ42-1 was added to the medium, and the extracellular solution was collected at 30 min after stimulation. A 50-μl sample was added to 50 μl of ATP assay mix containing luciferase-luciferin buffer. Luminescence was measured with a V3.1 Sirius luminometer (Berthold Detection Systems). A calibration curve (R^2, >0.996) was obtained from standard ATP samples, and the luminescence of the recording medium was measured as the background. The protein abundance in the cell lysate was used for normalization and was determined by using the Enhanced BCA protein assay kit (Beyotime, China).

Statistical methods. Statistical analysis was performed with SAS software (SAS Institute Inc., Cary, NC). Data are presented as means ± standard errors of the means (SEM). Statistical comparisons were assessed by one-way analysis of variance (ANOVA) with Tukey's test. Differences were considered to be significant at a P level of <0.05.

RESULTS

Nucleotides evoke pinocytosis in microglia. Microglial cells express a variety of purinergic receptors, some of which have been found related based on their physiological or pathological functions. To observe the effects of nucleotides on microglial motility, we developed an *in vitro* migration assay (11) and found unexpectedly that microglia formed large vacuoles at their leading edges in response to ATPγS, a nonhydrolyzable ATP homologue (Fig. 1A; see also Videos S1 and S2 in the supplemental material). When 100 μM ATPγS was repetitively pressure ejected into the microglial cultures through a pipette at a defined frequency and pulse duration to induce migration (11), resting microglia started to form stretch ruffles (sheet-like extensions of the plasma membrane) in minutes and migrated toward the pipette tip. The ruffles then closed, first into open cups and finally discrete vacuoles with diameters ranging from 0.5 to 5 μm (Fig. 1A; see also Fig. 3G, below, and Videos S1 and S2 in the supplemental material).

Phagosomes and pinosomes are both large membrane-bound compartments formed by cellular ingestion of extracellular materials (4, 5), and thus they became the candidates for the ATPγS-induced large vacuoles. Differentially, phagosomes are formed by direct zipper-like contacts between solid materials and cell membranes, while pinosomes are formed by enclosures of ruffling membranes induced by growth factors, involving the uptake of fluid-phase materials in large quantities (4, 5). To identify the ATPγS-induced large vacuoles, we used FD70S (fluorescein-dextrans with an average molecular weight of 70,000) as pinosomal markers (4, 17) and fluorescence-linked latex beads as phagosomal markers (4, 7). When cultured microglia were simultaneously treated with 100 μM ATPγS, 2 μg/μl FD70S, and fluorescence-labeled latex beads (0.004% solid; 0.5-μm diameter), ATPγS-induced vacuoles were selectively labeled by FD70S but rarely colocalized with the latex beads (Fig. 1B), indicating that the ATPγS-induced vacuoles were pinosomes. Moreover, ATPγS (100 μM) triggered a 4-fold increase in pinocytosis but only an ~30% increase in phagocytosis (Fig. 1C). Quantitative tests showed that ATPγS induced pinocytosis in a dose-dependent fashion in a 5-min incubation period (Fig. 1D and E). Statistically, both the intracellular fluorescence intensity and the pinosomal area of individual cells increased with exponentially increasing concentrations of ATPγS (Fig. 1E). Moreover, the ATPγS-induced internalization of FD70S was diminished by amiloride (Fig. 1F), an Na^+/H^+ exchanger blocker reported to selectively inhibit pinocytosis without disturbing other endocytotic pathways (18), confirming the ATPγS-induced pinocytosis. Interestingly, ATPγS only significantly induced pinocytosis in cultured microglia, and not in cultured astrocytes or neurons after an incubation period of 5 min (Fig. 1G). Taken together, these results demonstrate that ATPγS selectively evokes pinocytosis in cultured microglial cells.

$P2Y_4$ receptors mediate the ATPγS-induced microglial pinocytosis. We further identified the subtype of purinergic receptors responsible for the ATPγS-induced microglial pinocytosis. Since ATPγS is a potent P2Y receptor agonist (19), P2Y purinergic receptors are likely involved. RB2 and suramin, known as wide-spectrum antagonists of P2Y receptors (19), significantly inhibited the ATPγS-induced pinocytosis (Fig. 2A). Furthermore, we found that ATP (100 μM) or UTP (100 μM) triggered pinocytosis to an extent similar to that of ATPγS (Fig. 2B).

Among all the subtypes of rodent P2Y receptors, only $P2Y_2$ and $P2Y_4$ are activated by both UTP and ATP (19, 20). In addition, these receptors are differentially sensitive to RB2 and suramin. While $P2Y_4$ receptors are more sensitive to RB2 than to suramin, $P2Y_2$ receptors have the opposite sensitivity (19). Consistent with the involvement of $P2Y_4$, we found that RB2 at a relatively low

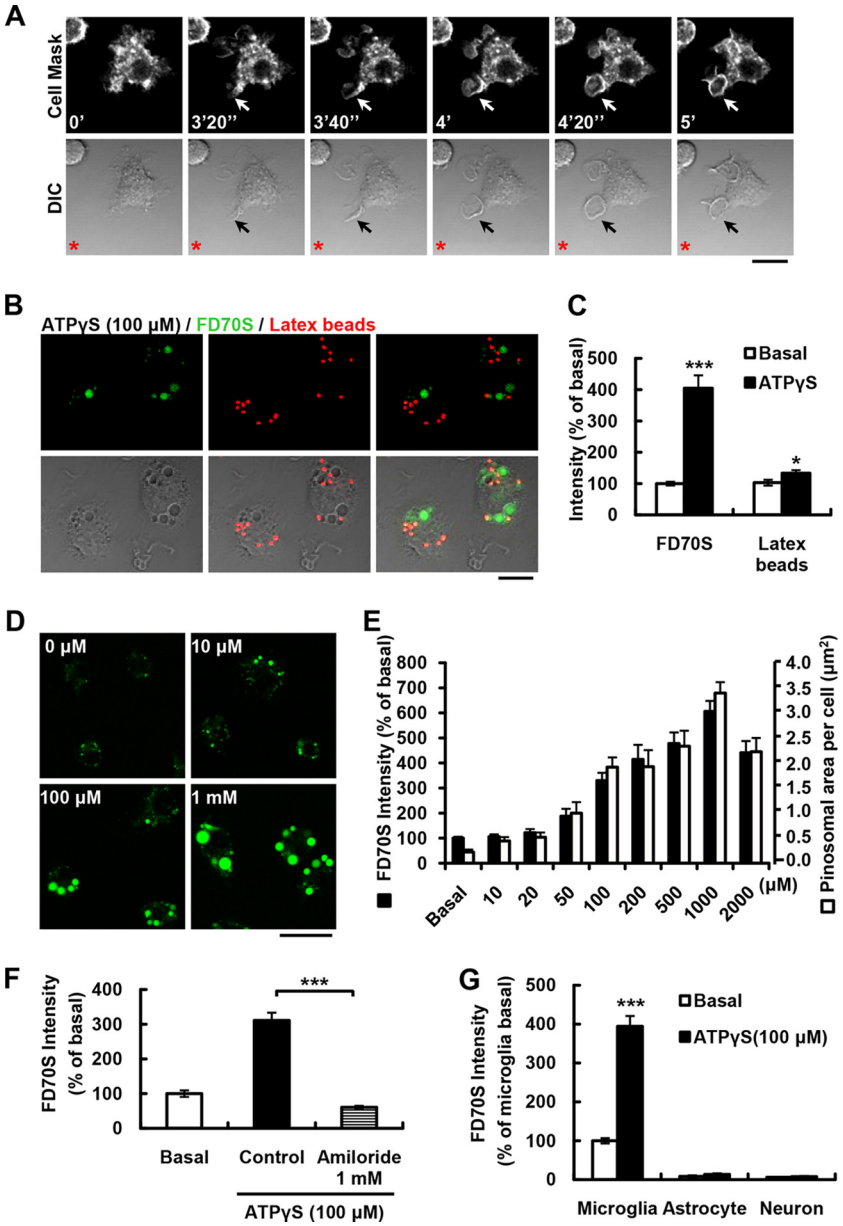

FIG 1 ATPγS-induced microglial pinocytosis. (A) Example images showing large vacuoles formed from dynamic membrane ruffles. The cell membrane was labeled by pretreatment with Cell Mask fluorescent dyes (1 μg/ml) for 3 min. ATPγS (100 μM) was added to the medium through a pipette positioned at the left bottom of the image (indicated by the asterisk). Arrows indicate membrane ruffles forming pinosomes. Times are indicated in minutes and seconds. Bar, 10 μm. (B) Example images showing that ATPγS-induced (100 μM, 5 min) pinosomes labeled by FD70S (green; 2 μg/μl) formed separately from phagosomes labeled with latex beads (red; 0.004%) in cultured microglia. Fluorescence images (upper panels) are superimposed on the DIC images in the lower panels. Bar, 10 μm. (C) Quantitative data from the results shown in panel B. The level of pinocytosis was evaluated as the intracellular fluorescence intensity of FD70S. The level of phagocytosis is represented as the number of beads internalized by individual cells. The value from microglia without ATPγS treatment was taken as basal (100%). (D) Examples of fluorescence images, showing the dose-dependent effects of ATPγS (5 min) on microglial pinocytosis (the label was FD70S at 2 μg/μl). The concentrations of ATPγS applied are indicated in each panel. Bar, 20 μm. (E) Summary of the dose dependence of ATPγS-induced pinocytosis in cultured microglia. The level of pinocytosis was evaluated as the intracellular fluorescence intensity or the total area of pinosomes inside individual cells. The concentrations of ATPγS applied are indicated on the *x* axis. Values from microglia treated with 2 μg/μl FD70S alone were taken as the basal control. (F) Amiloride (1 mM) inhibited ATPγS-induced (100 μM) pinocytosis of FD70S (2 μg/μl, 5 min). The fluorescence intensity represents the amount of FD70S internalized. (G) Summary data showing that no apparent spontaneous or ATPγS-induced (100 μM) FD70S (2 μg/μl, 5 min) uptake was observed in cultured neurons or astrocytes. Data are normalized to spontaneous FD70S uptake in cultured microglia. For all summary data, results are means and SEM from three independent experiments, ***, $P < 0.001$; *, $P < 0.05$ (ANOVA with Tukey's test).

concentration (20 μM) had a much stronger inhibitory effect than suramin (250 μM) on the ATPγS-induced pinocytosis. We then determined if P2Y$_4$ receptors were expressed in microglia. Previous studies had identified that microglia express mRNAs encoding P2Y$_4$ receptors (19, 21, 22). We confirmed the expression of the P2Y$_4$ receptor at the protein level by Western blotting (Fig. 2C). Interestingly, although both P2Y$_2$ and P2Y$_4$ receptors were diffusely distributed in resting microglia (Fig. 2D), P2Y$_4$ but not

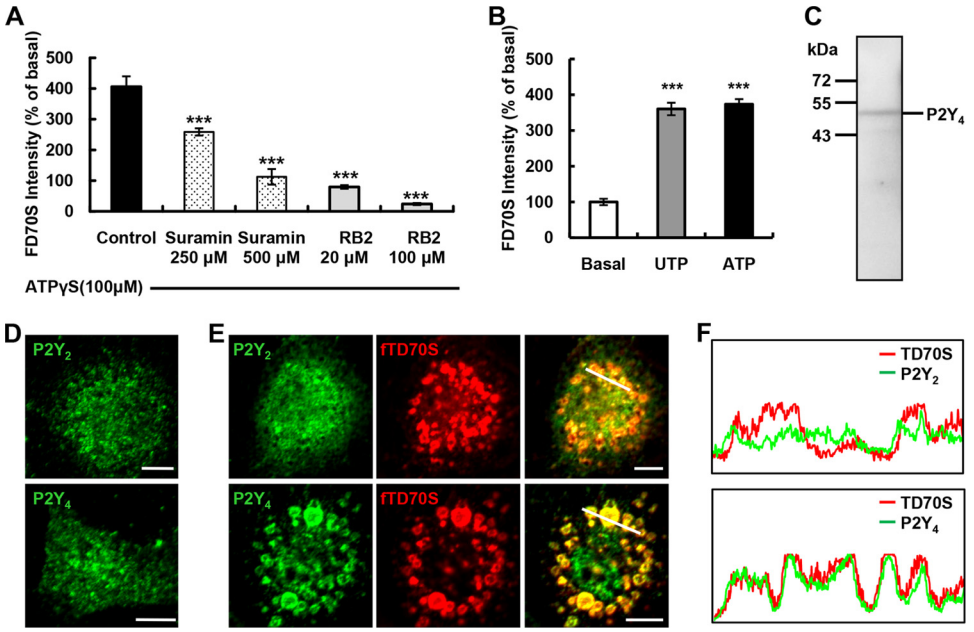

FIG 2 Involvement of $P2Y_4$ receptors in ATP-induced pinocytosis in cultured microglia. (A) Summary data of the differential inhibitory effects of $P2Y_4$ receptor antagonists (30-min pretreatment with different doses) on ATPγS-induced (100 μM, 5 min) pinosomes labeled with 2 μg/μl FD70S in cultured microglia. (B) Summary data showing that UTP (100 μM) had the same potency as ATP (100 μM) in inducing pinosomes labeled with 2 μg/μl FD70S for 5 min in cultured microglia. (C) Expression of $P2Y_4$ receptor protein confirmed by Western blotting. (D) Examples of immunostaining images, showing the diffuse distribution of $P2Y_2$ and $P2Y_4$ receptor expression in control cultured microglia. Bars, 10 μm. (E) Immunostaining of $P2Y_2$ (upper panels) and $P2Y_4$ (lower panels) receptors (green) in cultured microglia after treatment with ATPγS (100 μM) and fixable TD70S (2 μg/μl; red) for 5 min. The merged images show that the $P2Y_4$ immunostaining signal was colocalized with TD70S-labeled pinosomes. Bars, 10 μm. (F) Fluorescence intensity profile of a set of pixels distributed on the white lines drawn across pinosomes shown in the right merged images in panel E. The emission wavelengths corresponding to the signals of $P2Y_2$, $P2Y_4$, and TD70S are plotted. Data are presented in arbitrary units versus the length of the white line. For all summary data, results are means and SEM from three independent experiments, ***, $P < 0.001$ (ANOVA with Tukey's test).

$P2Y_2$ receptors tended to be associated with ATPγS-induced pinosomes (Fig. 2E and F).

To further address whether $P2Y_4$ receptors indeed mediated the ATPγS-induced pinocytosis, we designed a pool of siRNAs consisting of three oligonucleotide duplexes specific for rat $P2Y_4$ cDNA. The knockdown efficiencies of the siRNA pool and individual oligonucleotide of $P2Y_4$ receptors were confirmed in cultured astrocytes at the protein level by Western blotting (Fig. 3A) and at the RNA level by RT-PCR (Fig. 3B), respectively. We found that the ATPγS-induced pinocytosis was blocked in microglia transfected with the $P2Y_4$ siRNAs pool or with individual siRNAs but was not affected in cells transfected with control siRNA (Fig. 3E and F). $P2Y_2$ receptors have been found diffusely expressed in microglia and have an agonist spectrum similar to $P2Y_4$ receptors (Fig. 2B, E, and F). However, we found that siRNA specific for $P2Y_2$ receptors had no effect on pinocytosis in microglia (Fig. 3C, E, and F). Furthermore, an siRNA sequence specific for $P2Y_6$ receptors, which mediate phagocytosis in microglia (7), did not affect the ATPγS-induced pinocytosis (Fig. 3D, E, and F). We found that MRS2395, a specific $P2Y_{12}$ receptor antagonist, significantly inhibited microglial chemotaxis in the ATPγS gradient but had no impact on ATPγS-induced pinocytosis (Fig. 3G and H; see also Videos S2 and S3 in the supplemental material). Taken together, these results indicate a coupling between microglial $P2Y_4$ receptors and pinocytic activity.

Purine-mediated pinocytosis contributes to microglial clearance of soluble Aβ. Alzheimer's disease has been related to the accumulation of Aβ in the brain (23). Furthermore, soluble forms, rather than plaques, of Aβ have been identified to be key mediators in AD-related synaptic dysfunctions (24, 25). Microglia has been reported to internalize soluble Aβ through pinocytosis (26), although the underlying mechanism is still elusive. Since both fibrillar (27, 28) and soluble Aβ1-42 (27, 29) have been found to induce ATP release from microglia, we examined whether purine-mediated pinocytosis played a role in microglial clearance of soluble Aβ peptides and whether Aβ itself could induce pinocytosis in an ATP/P2Y receptor-dependent way. Indeed, ATPγS promoted microglial internalization of soluble Aβ (Fig. 4A). Furthermore, soluble Aβ peptides (Texas Red linked; 15 μM) and FD70S (Fig. 4B) were internalized into the same vacuoles in microglia after ATPγS treatment for 5 min, suggesting that soluble Aβ peptides were internalized via nucleotide-induced pinocytosis. We then clarified whether ATP and $P2Y_4$ receptors contributed to the spontaneous Aβ internalization by microglia. Apyrase (50 U/ml), an ATP-degrading enzyme (11), significantly decreased the spontaneous Aβ internalization (Fig. 4C). Furthermore, both $P2Y_4$ knockdown (Fig. 4D and E) and RB-2 (Fig. 4F) inhibited the spontaneous internalization of Texas Red-linked soluble Aβ (2 μM), while a $P2Y_6$ receptor antagonist had no effect (Fig. 4G and H). Consistent with previous studies, we found that Aβ1-42 (2 μM), but not the control peptide Aβ42-1, induced ATP release from microglia (Fig. 4I). Interestingly, another fragment of the Aβ peptide, Aβ1-40, also promoted ATP release, although with a weaker effect (Fig. 4I). These results suggested that ATP/$P2Y_4$ signaling mediates microglial internalization of soluble Aβ.

Interestingly, we found that incubation of soluble Aβ (100 μM,

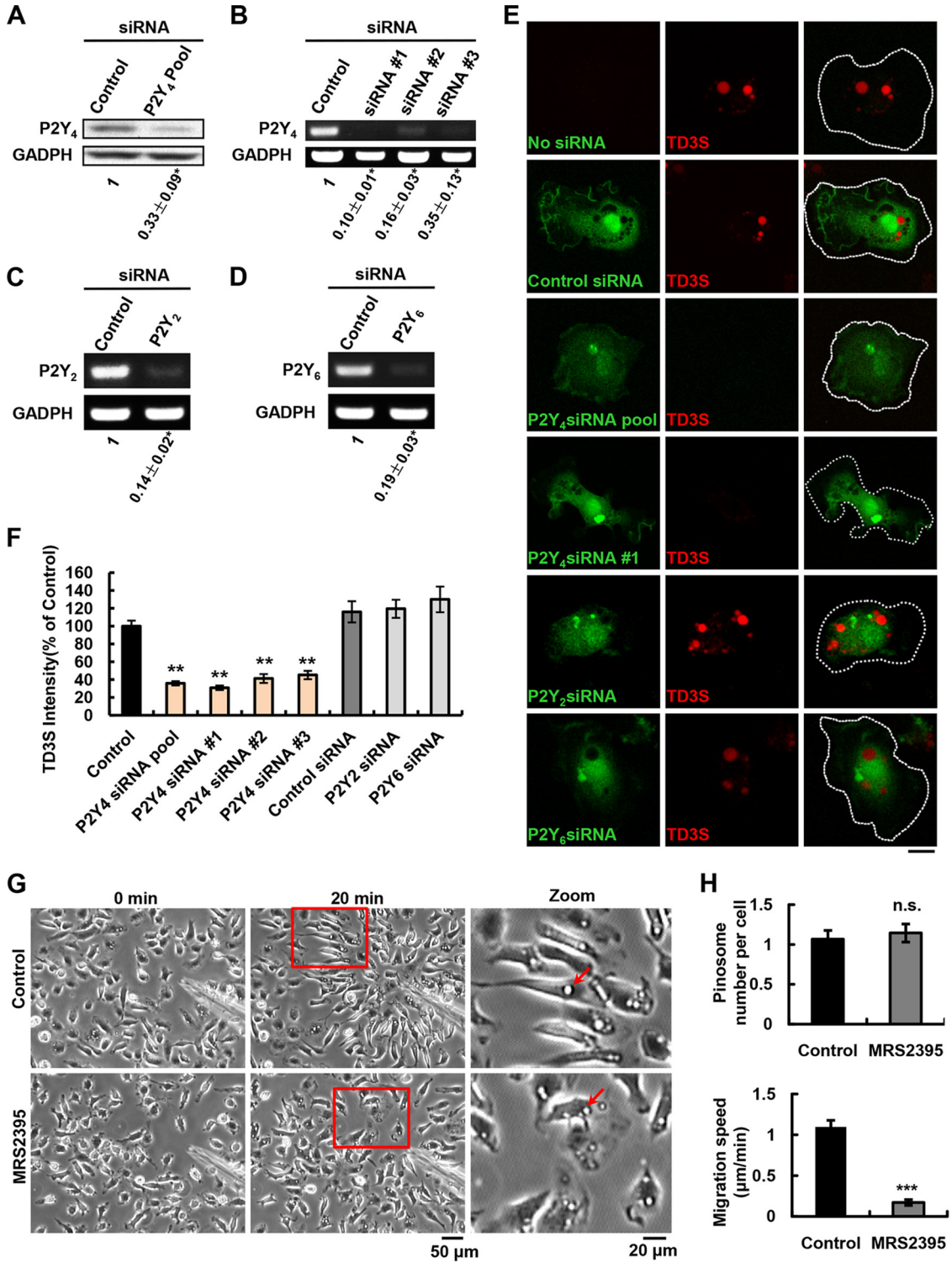

FIG 3 $P2Y_4$ receptors mediate ATPγS-induced microglial pinocytosis. (A) Western blots showing apparent downregulation of $P2Y_4$ receptor proteins in primary astrocytes cotransfected with an siRNA pool specific for the $P2Y_4$ receptors. (B to D) RT-PCR assay results, showing the knockdown efficiency in primary astrocytes transfected with three individual siRNAs contained in the $P2Y_4$ siRNA pool (B), siRNA specific for $P2Y_2$ (C), or siRNA specific for $P2Y_6$ (D). Numbers associated with each blot are averaged data ($n = 4$). (E) Examples of images showing the ATPγS-induced (100 μM) pinocytosis after labeling with TD3S (red; 2 μg/μl for 5 min) in control microglia (no siRNA) or microglia transfected with various siRNAs (green; the siRNA species are indicated in each panel) for 72 h. The dotted lines outline individual cells. Bars, 10 μm. (F) Quantitative data for the results shown in panel E. Values are the percentage of control (without siRNA transfection). (G) Examples of phase-contrast images, showing migration of cultured microglia toward the pipette tip at the center of the image field before (0 min) and 20 min after exposure to an ATPγS gradient created by pulsatile application (1 mM in the pipette) in the presence or absence of the $P2Y_{12}$ receptor antagonist MRS2395 (200 μM). Right panels, higher-magnification images of the red area in the middle panels, showing the ATPγS-induced pinosomes, which appeared as phase-bright vacuoles (indicated red arrows). (H) Quantitative data from the results shown in panel G, showing that MRS2395 largely blocked the microglial migration (lower panel) but failed to affect the microglial pinocytosis (upper panel) induced by ATPγS. For all summary data, results are means and SEM from three independent experiments. ***, $P < 0.001$; **, $P < 0.01$; *, $P < 0.05$; n.s., not significant (ANOVA with Tukey's test).

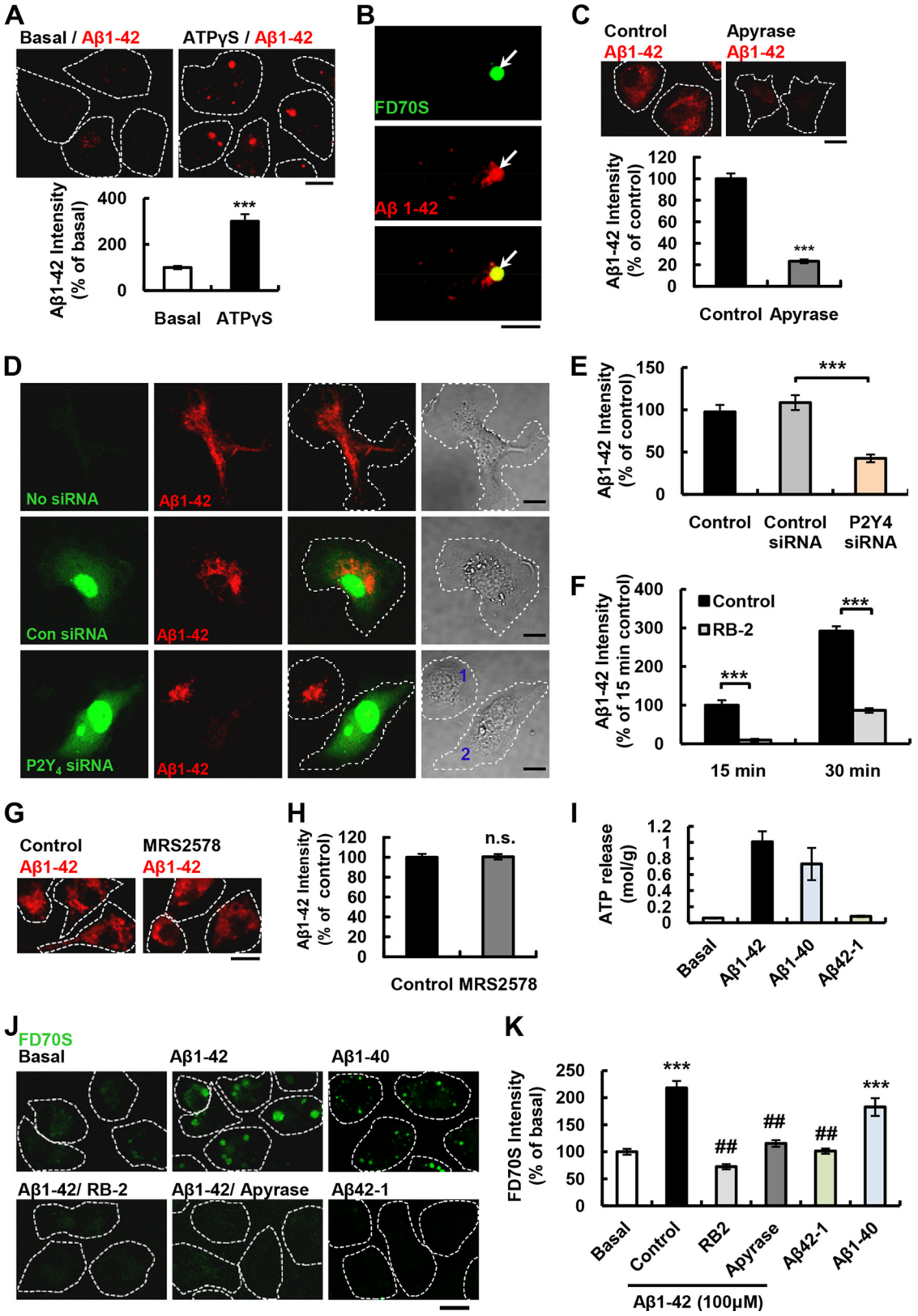

FIG 4 ATP-P2Y$_4$ signaling contributes to microglial pinocytosis of soluble Aβ1-42. (A) ATPγS (100 μM) enhanced internalization of Texas Red-linked Aβ1-42 (15 μM, 5 min; red) in cultured microglia. (Upper panels) Examples of fluorescence images. Dotted lines outline individual cells. Bar, 10 μm. (Lower panel) Summary data for ATPγS-induced Aβ1-42 internalization, presented as the fluorescence intensity of Texas Red-linked Aβ1-42. (B) Examples of images showing that ATPγS-induced (100 μM, 5 min) internalization of Texas Red-linked Aβ1-42 (15 μM; red) and FD70S (2 μg/μl; green) were distributed in the same pinosome (arrows). Bar, 10 μm. (C, upper panels) Fluorescence images showing that the microglial internalization of Texas Red-linked Aβ1-42 (red; 2 μM, 30

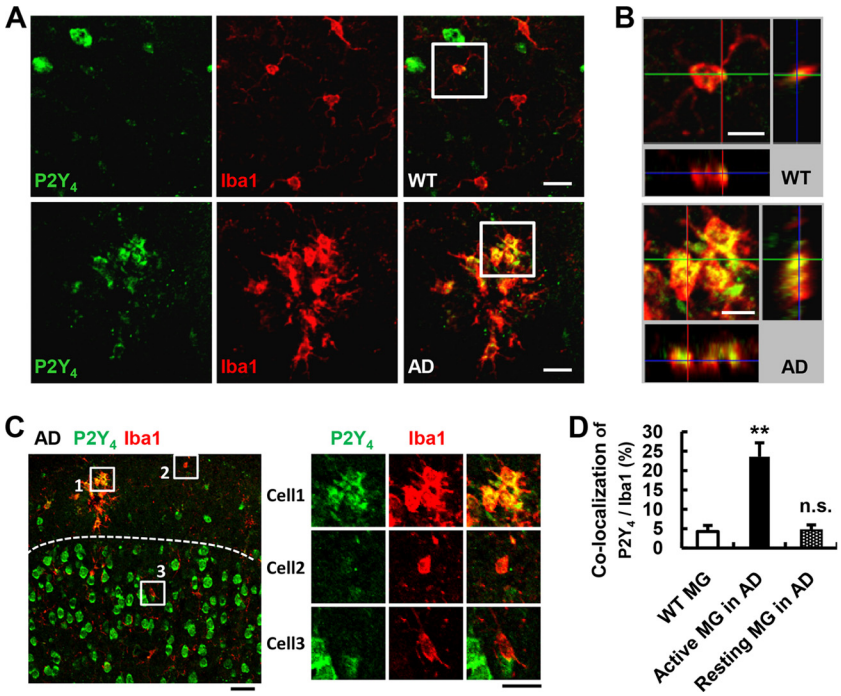

FIG 5 Increased expression of P2Y$_4$ receptors in AD mice. (A) Cerebral cortical sections prepared from 6-month-old wild-type mice (WT; upper panels) and APPswe/PS1dE9 mice (AD; lower panels) immunostained with anti-P2Y$_4$ (green) and anti-Iba1 (red) antibodies. Bars, 20 μm. (B) Higher-magnification images from the boxed areas of the merged images in panel A. *x-y* (top), *x-z* (bottom), and *y-z* (right) projections of immunostained sections from WT (upper panels) and APPswe/PS1dE9 (AD, lower panels) mice, in which the colocalization of the anti-P2Y$_4$ signal with the microglial marker Iba1 was further confirmed. Bar, 10 μm. (C, left) Lower-magnification image of the same brain slice as shown in panel A bottom images, to show a more extensive area. Bars, 40 μm. (Right) Higher-magnification images from the boxed areas of the merged images on the left. Dotted lines separate layer 1 (upper) and layers 2/3 (lower). Cell 1, cell 2, and cell 3 (also the example cells in panels A and B), corresponding to boxed areas 1, 2, and 3, respectively. Bars, 20 μm. (D) Quantitative summary of the colocalization of anti-P2Y$_4$ with anti-Iba1 signals (P2Y$_4$/Iba1), as shown in the images in panels A and C. Average P2Y$_4$ immunoreactivity per microglial cell was measured to evaluate the expression level of P2Y$_4$ (Iba1-positive cells) in WT and AD mouse brain sections. MG, microglia. Results are presented as means and SEM. **, $P < 0.01$; n.s. not significant (ANOVA with Tukey's test).

5 min) promoted FD70S endocytosis (Fig. 4J and K), suggesting that Aβ itself induces pinocytosis. In addition, Aβ1-40 but not the control peptide Aβ42-1 also stimulated pinosome formation (Fig. 4J and K). The Aβ-induced pinocytosis of FD70S was significantly inhibited by the P2Y receptor antagonist RB-2 and the ATP-degrading enzyme apyrase (Fig. 4J and K). The evidence that apyrase blocked Aβ peptide-induced pinocytosis indicates that Aβ-induced pinocytosis requires extracellular ATP, and Aβ itself is not a direct agonist for P2Y receptors. Our results suggest that pinocytosis of Aβ in microglia is an ATP-regulated active process, rather than a spontaneous passive activity.

Microglial cells are known to exist in two forms, resting and reactive (1). In healthy brains, microglial cells are predominately ramified resting cells with a small cell body and multiple processes that detect the environment (30). In response to various pathological insults, microglial cells can transform into amoeboid reactive forms with a larger cell body and fewer processes (1, 31). Accumulation of amoeboid-like reactive microglial cells at the beta amyloid aggregations is a hallmark of the AD brain (32, 33). We found that although immunostaining detected a low expression level of P2Y$_4$ receptors in the resting microglia in the control mouse brain, strong anti-P2Y$_4$ immunostain signaling was detected in the accumulated reactive microglia in the brain of APPswe/PS1dE9 mouse mutant, the mouse model of AD (Fig. 5A, B, and D; see also Videos S4 and S5 in the supplemental material). Interestingly, strong P2Y$_4$ immunostaining was observed only in

min) was inhibited by apyrase (50 U/ml). (Lower panel) Quantitative summary of results presented in the upper panels. (D) Examples of images showing the internalization of Texas Red-linked Aβ1-42 (red; 2 μM, 30 min) in control microglia or in microglia transfected with control siRNA or P2Y$_4$ siRNA (green). Note that in the bottom panels, Aβ1-42 was internalized by an untransfected cell (cell 1) but not its neighbor (cell 2), which was transfected with P2Y$_4$ pooled siRNA (green). Bar, 10 μm. (E) Quantitative data for the results shown in panel D. Values are the percentage of the control (without siRNA transfection). (F) The P2Y antagonist RB2 (20 μM) inhibited the uptake of FAM-linked Aβ1-42 (2 μM) in cultured microglia. (G and H) Microglial internalization of Texas Red-linked Aβ1-42 (red; 2 μM, 30 min) was not affected by the P2Y$_6$ antagonist MRS2578 (2 μM). (H) Quantitative summary of the results shown in panel G. (I) Determination of ATP release from microglia treated with Aβ1-42 (2 μM), Aβ1-40 (2 μM), or Aβ42-1 (2 μM). Values of ATP (in moles) were normalized to the protein abundance of cell lysates (in grams). (J) Examples of microscopic images of Aβ1-42-induced (100 μM; upper middle panel) pinosomes labeled with FD70S (2 μg/μl; green) in cultured microglia. Results with cells treated with FD70S only (upper left panel) were taken as the basal response. Both the P2Y receptor antagonist RB-2 (20 μM; lower left panel) and the ATP-degrading enzyme apyrase (50 U/ml; lower middle panel) blocked the Aβ1-42-induced FD70S internalization. Aβ1-40 (100 μM; upper right panel), but not Aβ 42-1 (100 μM; lower right panel), also induced pinocytosis in microglia. (K) Quantitative summary of the results shown in panel J. ***, $P < 0.001$, compared with data from basal; ##, $P < 0.01$, compared with data from Aβ1-42-treated microglia. For all summary data, results are means and SEM from three independent experiments. ***, $P < 0.001$; n.s., not significant (ANOVA with Tukey's test).

the aggregated reactive microglia, and not in the diffusely distributed resting microglia in the mutant mouse (Fig. 5C). These results may reflect a chronic homeostatic change in the microglial Aβ uptake capacity to adapt to the prolonged increase in extracellular Aβ peptide. A similar increase in $P2Y_6$ receptor expression in reactive microglia has been reported in injured brains (7).

The PI3K/Akt pathway is involved in microglial pinocytosis. PI3K has been reported to be crucial in the completion of pinocytosis induced by macrophage colony-stimulating factor (17). We found that PI3K inhibitors, either wortmannin (500 nM) or LY294002 (50 μM), drastically reduced ATPγS-induced pinocytosis (Fig. 6A). In addition, both inhibitors blocked the Aβ-induced pinocytosis (Fig. 6B) as well as the spontaneous soluble Aβ internalization (Fig. 6C), indicating the requirement for PI3K in both processes. As a major downstream target of PI3K, phosphorylated Akt represents the activation level of the PI3K/Akt signaling pathway (34). We found that application of 100 μM ATPγS rapidly promoted Akt phosphorylation (Fig. 6D). In addition, an antiphosphorylated Akt signal, but not the anti-total Akt immunostaining signal, was observed to accumulate on membrane ruffles and newly formed pinosomes (Fig. 6E, lower panel), although in the resting state, both the total and phosphorylated Akt signals were diffusely distributed throughout the whole cell (Fig. 6E, upper panel). In accordance with the Aβ-induced pinocytosis (Fig. 4J and K), application of soluble Aβ1-42, at a concentration of either 2 μM, 20 μM, or 100 μM, promoted Akt phosphorylation (Fig. 6F) with a similar time course as with ATPγS (Fig. 6D). Aβ1-40, but not the control peptide Aβ42-1, also promoted Akt phosphorylation (Fig. 6G). Moreover, treatment of apyrase, RB-2, or LY294002 suppressed the Aβ-induced Akt phosphorylation (Fig. 6H and I). Taken together, these results indicate that activation of the PI3K/Akt cascade is involved in the P2Y receptor-mediated pinocytosis and contributes to the Aβ-induced self-uptake by microglia.

DISCUSSION

ATP functions as a "drink me" signal through activation of $P2Y_4$ receptors. Nucleotides are crucial signaling messengers in both neurons and glia in the CNS (13, 19, 35). Purinergic receptors are classified into P1 receptors, which are activated by nucleosides, and P2 receptors, which are activated by nucleotides (19). P2 receptors are further divided into P2X (ligand-gated ion channel receptors) and P2Y (G-protein-coupled receptors), both of which include multiple subtypes (19). Through the activation of multiple subtypes of purinergic receptors on microglia, purines induce complicated microglial responses, including chemotaxis, phagocytosis, and cytokine release, actions that play critical roles in pathological activities, such as neuronal injury, inflammation, and neuropathic pain. For example, activation of $P2X_4$ and $P2X_7$ receptors has been linked to microglial cytokine release to induce neuropathic pain after peripheral nerve injury (19). In addition, ATP has been proposed as a "find me" signal for inducing microglial migration through the activation of $P2Y_{12}$ receptors (8–10), whereas UDP acts as an "eat me" signal for triggering microglia phagocytosis through the activation of $P2Y_6$ receptors (7). Cohn and Parks reported that purines are efficient triggers for pinocytosis in macrophages (36), but the underlying mechanisms are not clear.

The $P2Y_4$ receptor is expressed in both neurons and glial cells, whereas its physiological function is largely unknown (37). In the present study, we demonstrated in microglia that ATP robustly induced pinocytosis (Fig. 1), with only a mild effect on phagocytosis (Fig. 1B and C). Our results demonstrated ATP as a "drink me" signal for microglial pinocytosis through the activation of $P2Y_4$ receptors (Fig. 7).

Signal transduction mechanisms in $P2Y_4$ receptor-mediated pinocytosis. Activation of PI3K at the plasma membrane has been found to be related to the growth factor-induced cytoskeletal remodeling and membrane ruffling that leads to increased pinocytosis (17, 38). Our findings revealed the requirement of activated PI3K/Akt signaling in $P2Y_4$ receptor-mediated pinocytosis (Fig. 6A, D, and E) as well as in $P2Y_4$ receptor-mediated microglial clearance of Aβ1-42 (Fig. 6B, C, and F). $P2Y_4$ receptors may activate PI3K/Akt signaling directly, as has been revealed for some G_q-coupled receptors (39, 40), a group to which the $P2Y_4$ receptor also belongs (41). The cross talk between G protein-coupled receptors (GPCRs) and growth factor receptors at their downstream signaling transduction pathways, including the PI3K/Akt cascade, has been well illustrated (40, 42, 43). GPCRs vary between each other. Drugs that target GPCRs are directed toward only a few GPCR members and thus may have fewer side effects and better therapeutic benefits than those targeting growth factor receptors. Therefore, the replacement of growth factor receptors by GPCRs as drug targets may provide promising opportunities for drug discovery (42).

The finding that the diffusely distributed $P2Y_4$ receptors in microglia became associated with pinosomes after treatment with 100 μM ATPγS (Fig. 2E and F) indicated that, like the internalization of epidermal growth factor (EGF) receptors via pinocytic ruffles when exposed to a high concentration of EGF (5), $P2Y_4$ receptors on the microglial plasma membrane may also be internalized through pinocytic activity, leading to rapid feedback control of the cellular sensitivity to extracellular purines.

Aβ peptide-induced self-uptake through microglial pinocytosis mediated by autocrine ATP signaling. Aβ is normally generated at high levels in the brain and must be cleared at an equivalent rate (44). Accumulating evidence indicates that microglia play a critical role in the clearance of both soluble and fibrillar forms of Aβ through multiple mechanisms (45). The fibrillar forms can be taken up by phagocytosis through interaction with a cell surface's innate immune receptor complex (45). Recent studies have identified important roles of microglial pinocytosis in the internalization of soluble Aβ peptides (26). However, the mechanism underlying the microglial clearance of soluble Aβ is largely unknown. Pinocytosis, the most effective way for cells to ingest large amounts of extracellular fluid, is involved in a number of physiological and pathological processes, including the sampling of soluble antigens (46) and the uptake of nutrients (47). Consistent with the previous study (26), we found that microglia took up soluble Aβ by pinocytosis (Fig. 4B). We further identified that in microglia ATP was sufficient to promote Aβ uptake (Fig. 4A and B) and that activation of $P2Y_4$ receptors was necessary for Aβ uptake (Fig. 4C, D, E, and F). Notably, in accordance with the previous report that microglia is much more efficient in Aβ uptake than astrocytes and neurons (26), ATPγS only significantly induced pinocytosis in cultured microglia, and not in cultured astrocytes or neurons (Fig. 1G).

Interestingly, we found that Aβ peptide itself triggered pinocytosis in an ATP/P2Y-dependent manner (Fig. 4J and K). These results suggest that pinocytosis of Aβ by microglia is an active and

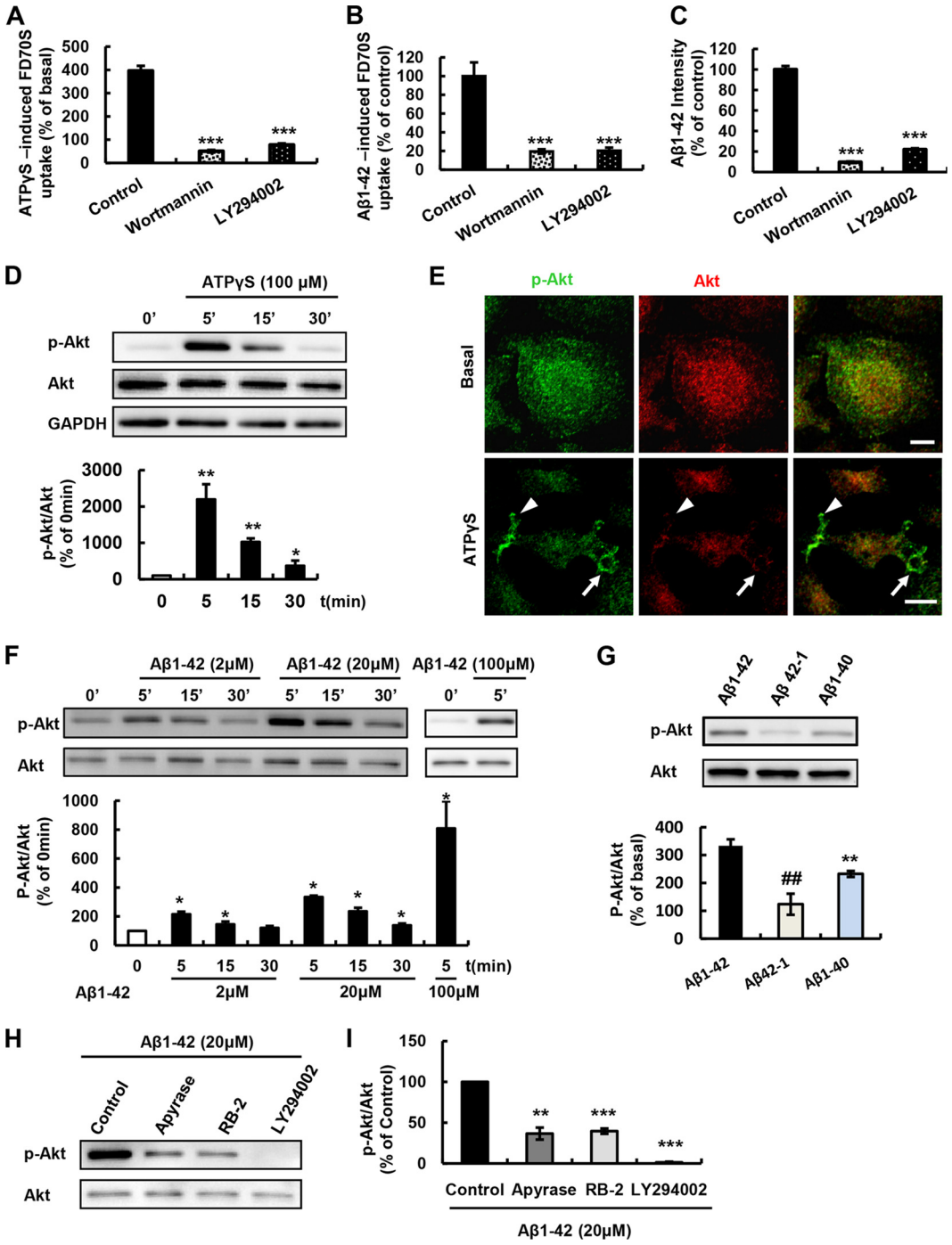

FIG 6 The PI3K/Akt pathway contributes to the microglial pinocytosis induced by ATPγS and the microglial internalization of soluble Aβ1-42. (A) Summary data of ATPγS-induced pinocytosis in the absence or presence of PI3 kinase inhibitors. Cultured microglia were preincubated with wortmannin (500 nM) or LY294002 (50 μM) for 30 min and then treated with 100 μM ATPγS and 2 μg/μl FD70S for 5 min. (B) Summary data of the Aβ1-42 (100 μM)-induced pinocytosis in the absence or presence of PI3 kinase inhibitors. Cultured microglia were preincubated with wortmannin (500 nM) or LY294002 (50 μM) for 30 min and then treated with 100 μM Aβ1-42 and 2 μg/μl FD70S for 5 min. (C) Summary data for spontaneous microglial uptake of soluble Aβ1-42 in the absence or presence of PI3 kinase inhibitors. Cultured microglia were preincubated with wortmannin (500 nM) or LY294002 (50 μM) for 30 min and then treated with 2 μM Texas Red-linked Aβ1-42 for 30 min. (D) Time-dependent effects of ATPγS (100 μM) on Ser-473 phosphorylation of Akt (p-Akt), as determined with Western blotting. Results were standardized to total Akt (p-Akt) and are expressed as p-Akt/Akt relative to the baseline. (E) Distribution of p-Akt (green) and Akt (red), shown by immunostaining results for cultured microglia with or without 100 μM ATPγS treatment for 5 min. Note that p-Akt accumulated at the newly formed membrane ruffles (arrowheads) and pinosomes (arrows) after treatment with ATPγS. Bars, 10 μm. (F) Time- and dose-dependent effects of Aβ1-42 (2 μM, 20 μM, or 100 μM) on Ser-473 phosphorylation of Akt (p-Akt). Western blotting results are shown at the top. (G) Effects of Aβ1-40 (20 μM) or Aβ42-1 (20 μM) on Ser-473 phosphorylation of Akt (p-Akt). Western blotting results are shown at the top. **, $P < 0.01$, compared with data from basal; ##, $P < 0.01$, compared with data from Aβ1-42-treated microglia. (H and I) Suppression of Aβ1-42-induced (20 μM) Akt phosphorylation (p-Akt) by apyrase (50 U/ml), RB-2 (25 μM), and LY294002 (50 μM). (I) Summary of Western blotting results shown in panel H. For all summary data, results are means and SEM from three independent experiments. ***, $P < 0.00$; **, $P < 0.01$; *, $P < 0.05$ (ANOVA with Tukey's test).

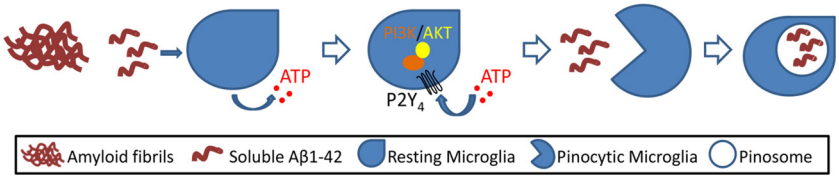

FIG 7 A cartoon model showing that soluble Aβ1-42 is taken up by microglia through an autocrine loop via ATP/$P2Y_4$-regulated pinocytosis.

regulated activity rather than a spontaneous and constitutive process. Our results suggest that ATP endogenously released from Aβ-stimulated microglia works as an autocrine signal to evoke pinocytosis, leading to their clearance of Aβ peptides in the brain (Fig. 7). Still, the *in vivo* physiological significance of our findings remains to be established.

It should be noted that the Aβ-induced ATP release may not be limited to microglia. A recent study reported that astrocyte-secreted ATP in response to amyloid beta protected against the Aβ1-42-induced impairment of synaptic plasticity by restoring the Aβ1-42-mediated reduction of synaptic proteins, including NR2A and PSD-95 (48). How Aβ1-42 induces ATP release from glial cells is largely unknown. Lysosomal exocytosis of ATP has been reported for several types of glial cells or monocytes induced under various conditions (11, 35, 49–51). Whether the Aβ1-42-induced ATP release in glial cells is also through lysosomal exocytosis needs further clarification.

The distribution pattern of Aβ is different between ATPγS-induced Aβ uptake and spontaneous Aβ internalization. The spontaneous Aβ uptake is likely through pinosomes of small sizes, in accordance with the evidence that Aβ at 2 μM caused a relatively weaker promotion of Akt phosphorylation (Fig. 6E) than ATPγS did (Fig. 6C) and that the pinosomal area is dose dependent on the ATPγS concentration (Fig. 1D and E).

In contrast to the previous view, recent studies have shown that resting microglia dynamically extend and retract their processes to actively survey the surrounding environment (52, 53). Interestingly, the processes of resting microglia make frequent contact with synapses in a neuronal activity-dependent manner, suggesting that they constantly monitor the functional status of synapses (54–56). Since soluble Aβ is released from presynaptic terminals (57) and is toxic to synapses when it accumulates extracellularly (24, 58), the Aβ-triggered self-uptake through microglial pinocytosis evoked by an autocrine ATP signal induced by Aβ itself may play a role in preventing Aβ-induced synaptic dysfunction and synapse loss. Since there is currently no methodology to accurately detect the local concentration of amyloid beta in the brain, it is unclear whether the concentration of amyloid beta at the site of synapse is sufficient to induce microglial activities. More in-depth studies are needed to identify the *in vivo* function of purine-mediated microglia-neuron cross talk.

ACKNOWLEDGMENTS

We thank I. C. Bruce for critical comments on the manuscript.

This work was supported by grants from the Major State Basic Research Program of China (2011CB504400), the National Natural Science Foundation of China (31190060, 81221003, 30730037, and 30870834), and PCSIRT.

REFERENCES

1. **Barron KD.** 1995. The microglial cell: a historical review. J. Neurol. Sci. **134**(Suppl):57–68.
2. **Raivich G.** 2005. Like cops on the beat: the active role of resting microglia. Trends Neurosci. **28:**571–573.
3. **Rivest S.** 2009. Regulation of innate immune responses in the brain. Nat. Rev. Immunol. **9:**429–439.
4. **Swanson JA.** 2008. Shaping cups into phagosomes and macropinosomes. Nat. Rev. Mol. Cell Biol. **9:**639–649.
5. **Doherty GJ, McMahon HT.** 2009. Mechanisms of endocytosis. Annu. Rev. Biochem. **78:**857–902.
6. **Lauber K, Bohn E, Krober SM, Xiao YJ, Blumenthal SG, Lindemann RK, Marini P, Wiedig C, Zobywalski A, Baksh S, Xu Y, Autenrieth IB, Schulze-Osthoff K, Belka C, Stuhler G, Wesselborg S.** 2003. Apoptotic cells induce migration of phagocytes via caspase-3-mediated release of a lipid attraction signal. Cell **113:**717–730.
7. **Koizumi S, Shigemoto-Mogami Y, Nasu-Tada K, Shinozaki Y, Ohsawa K, Tsuda M, Joshi BV, Jacobson KA, Kohsaka S, Inoue K.** 2007. UDP acting at P2Y6 receptors is a mediator of microglial phagocytosis. Nature **446:**1091–1095.
8. **Davalos D, Grutzendler J, Yang G, Kim JV, Zuo Y, Jung S, Littman DR, Dustin ML, Gan WB.** 2005. ATP mediates rapid microglial response to local brain injury in vivo. Nat. Neurosci. **8:**752–758.
9. **Haynes SE, Hollopeter G, Yang G, Kurpius D, Dailey ME, Gan WB, Julius D.** 2006. The P2Y12 receptor regulates microglial activation by extracellular nucleotides. Nat. Neurosci. **9:**1512–1519.
10. **Honda S, Sasaki Y, Ohsawa K, Imai Y, Nakamura Y, Inoue K, Kohsaka S.** 2001. Extracellular ATP or ADP induce chemotaxis of cultured microglia through $G_{i/o}$-coupled P2Y receptors. J. Neurosci. **21:**1975–1982.
11. **Dou Y, Wu HJ, Li HQ, Qin S, Wang YE, Li J, Lou HF, Chen Z, Li XM, Luo QM, Duan S.** 2012. Microglial migration mediated by ATP-induced ATP release from lysosomes. Cell Res. **22:**1022–1033.
12. **Galea E, Feinstein DL.** 1992. Rapid synthesis of DNA deletion constructs for mRNA quantitation: analysis of astrocyte mRNAs. PCR Methods Appl. **2:**66–69.
13. **Zhang JM, Wang HK, Ye CQ, Ge W, Chen Y, Jiang ZL, Wu CP, Poo MM, Duan S.** 2003. ATP released by astrocytes mediates glutamatergic activity-dependent heterosynaptic suppression. Neuron **40:**971–982.
14. **Guan CB, Xu HT, Jin M, Yuan XB, Poo MM.** 2007. Long-range Ca2+ signaling from growth cone to soma mediates reversal of neuronal migration induced by slit-2. Cell **129:**385–395.
15. **Fire A, Xu S, Montgomery MK, Kostas SA, Driver SE, Mello CC.** 1998. Potent and specific genetic interference by double-stranded RNA in Caenorhabditis elegans. Nature **391:**806–811.
16. **Mello CC, Conte D, Jr.** 2004. Revealing the world of RNA interference. Nature **431:**338–342.
17. **Araki N, Johnson MT, Swanson JA.** 1996. A role for phosphoinositide 3-kinase in the completion of macropinocytosis and phagocytosis by macrophages. J. Cell Biol. **135:**1249–1260.
18. **Koivusalo M, Welch C, Hayashi H, Scott CC, Kim M, Alexander T, Touret N, Hahn KM, Grinstein S.** 2010. Amiloride inhibits macropinocytosis by lowering submembranous pH and preventing Rac1 and Cdc42 signaling. J. Cell Biol. **188:**547–563.
19. **Fields RD, Burnstock G.** 2006. Purinergic signalling in neuron-glia interactions. Nat. Rev. Neurosci. **7:**423–436.
20. **Wildman SS, Unwin RJ, King BF.** 2003. Extended pharmacological profiles of rat P2Y2 and rat P2Y4 receptors and their sensitivity to extracellular H+ and Zn2+ ions. Br. J. Pharmacol. **140:**1177–1186.
21. **Crain JM, Nikodemova M, Watters JJ.** 2009. Expression of P2 nucleotide receptors varies with age and sex in murine brain microglia. J. Neuroinflammation **6:**24. doi:10.1186/1742-2094-6-24.
22. **Seo DR, Kim SY, Kim KY, Lee HG, Moon JH, Lee JS, Lee SH, Kim SU, Lee YB.** 2008. Cross talk between P2 purinergic receptors modulates extracellular ATP-mediated interleukin-10 production in rat microglial cells. Exp. Mol. Med. **40:**19–26.

23. **Hardy J, Selkoe DJ.** 2002. The amyloid hypothesis of Alzheimer's disease: progress and problems on the road to therapeutics. Science **297:**353–356.
24. **Hsia AY, Masliah E, McConlogue L, Yu GQ, Tatsuno G, Hu K, Kholodenko D, Malenka RC, Nicoll RA, Mucke L.** 1999. Plaque-independent disruption of neural circuits in Alzheimer's disease mouse models. Proc. Natl. Acad. Sci. U. S. A. **96:**3228–3233.
25. **Lauren J, Gimbel DA, Nygaard HB, Gilbert JW, Strittmatter SM.** 2009. Cellular prion protein mediates impairment of synaptic plasticity by amyloid-beta oligomers. Nature **457:**1128–1132.
26. **Mandrekar S, Jiang Q, Lee CY, Koenigsknecht-Talboo J, Holtzman DM, Landreth GE.** 2009. Microglia mediate the clearance of soluble Aβ through fluid phase macropinocytosis. J. Neurosci. **29:**4252–4262.
27. **Kim HJ, Ajit D, Peterson TS, Wang Y, Camden JM, Gibson Wood W, Sun GY, Erb L, Petris M, Weisman GA.** 2012. Nucleotides released from $A\beta_{1-42}$-treated microglial cells increase cell migration and $A\beta_{1-42}$ uptake through $P2Y_2$ receptor activation. J. Neurochem. **121:**228–238.
28. **Kim SY, Moon JH, Lee HG, Kim SU, Lee YB.** 2007. ATP released from beta-amyloid-stimulated microglia induces reactive oxygen species production in an autocrine fashion. Exp. Mol. Med. **39:**820–827.
29. **Sanz JM, Chiozzi P, Ferrari D, Colaianna M, Idzko M, Falzoni S, Fellin R, Trabace L, Di Virgilio F.** 2009. Activation of microglia by amyloid β requires P2X7 receptor expression. J. Immunol. **182:**4378–4385.
30. **Bero AW, Yan P, Roh JH, Cirrito JR, Stewart FR, Raichle ME, Lee JM, Holtzman DM.** 2011. Neuronal activity regulates the regional vulnerability to amyloid-beta deposition. Nat. Neurosci. **14:**750–756.
31. **Orr AG, Orr AL, Li XJ, Gross RE, Traynelis SF.** 2009. Adenosine A(2A) receptor mediates microglial process retraction. Nat. Neurosci. **12:**872–878.
32. **Bolmont T, Haiss F, Eicke D, Radde R, Mathis CA, Klunk WE, Kohsaka S, Jucker M, Calhoun ME.** 2008. Dynamics of the microglial/amyloid interaction indicate a role in plaque maintenance. J. Neurosci. **28:**4283–4292.
33. **Giulian D, Haverkamp LJ, Li J, Karshin WL, Yu J, Tom D, Li X, Kirkpatrick JB.** 1995. Senile plaques stimulate microglia to release a neurotoxin found in Alzheimer brain. Neurochem. Int. **27:**119–137.
34. **Hennessy BT, Smith DL, Ram PT, Lu Y, Mills GB.** 2005. Exploiting the PI3K/AKT pathway for cancer drug discovery. Nat. Rev. Drug Discov. **4:**988–1004.
35. **Zhang Z, Chen G, Zhou W, Song A, Xu T, Luo Q, Wang W, Gu XS, Duan S.** 2007. Regulated ATP release from astrocytes through lysosome exocytosis. Nat. Cell Biol. **9:**945–953.
36. **Cohn ZA, Parks E.** 1967. The regulation of pinocytosis in mouse macrophages. 3. The induction of vesicle formation by nucleosides and nucleotides. J. Exp. Med. **125:**457–466.
37. **Song X, Guo W, Yu Q, Liu X, Xiang Z, He C, Burnstock G.** 2011. Regional expression of P2Y(4) receptors in the rat central nervous system. Purinergic Signal. **7:**469–488.
38. **Rupper A, Lee K, Knecht D, Cardelli J.** 2001. Sequential activities of phosphoinositide 3-kinase, PKB/Aakt, and Rab7 during macropinosome formation in Dictyostelium. Mol. Biol. Cell **12:**2813–2824.
39. **Dugourd C, Gervais M, Corvol P, Monnot C.** 2003. Akt is a major downstream target of PI3-kinase involved in angiotensin II-induced proliferation. Hypertension **41:**882–890.
40. **Gosens R, Zaagsma J, Grootte Bromhaar M, Nelemans A, Meurs H.** 2004. Acetylcholine: a novel regulator of airway smooth muscle remodelling? Eur. J. Pharmacol. **500:**193–201.
41. **Communi D, Motte S, Boeynaems JM, Pirotton S.** 1996. Pharmacological characterization of the human P2Y4 receptor. Eur. J. Pharmacol. **317:**383–389.
42. **Lappano R, Maggiolini M.** 2011. G protein-coupled receptors: novel targets for drug discovery in cancer. Nat. Rev. Drug Discov. **10:**47–60.
43. **Taboubi S, Garrouste F, Parat F, Pommier G, Faure E, Monferran S, Kovacic H, Lehmann M.** 2010. G_q-coupled purinergic receptors inhibit insulin-like growth factor-I/phosphoinositide 3-kinase pathway-dependent keratinocyte migration. Mol. Biol. Cell **21:**946–955.
44. **Bateman RJ, Munsell LY, Morris JC, Swarm R, Yarasheski KE, Holtzman DM.** 2006. Human amyloid-beta synthesis and clearance rates as measured in cerebrospinal fluid in vivo. Nat. Med. **12:**856–861.
45. **Lee CY, Landreth GE.** 2010. The role of microglia in amyloid clearance from the AD brain. J. Neural Transm. **117:**949–960.
46. **Sallusto F, Cella M, Danieli C, Lanzavecchia A.** 1995. Dendritic cells use macropinocytosis and the mannose receptor to concentrate macromolecules in the major histocompatibility complex class II compartment: downregulation by cytokines and bacterial products. J. Exp. Med. **182:**389–400.
47. **Cardelli J.** 2001. Phagocytosis and macropinocytosis in Dictyostelium: phosphoinositide-based processes, biochemically distinct. Traffic **2:**311–320.
48. **Jung ES, An K, Hong HS, Kim JH, Mook-Jung I.** 2012. Astrocyte-originated ATP protects Aβ(1-42)-induced impairment of synaptic plasticity. J. Neurosci. **32:**3081–3087.
49. **Shin YH, Lee SJ, Jung J.** 2012. Secretion of ATP from Schwann cells through lysosomal exocytosis during Wallerian degeneration. Biochem. Biophys. Res. Commun. **429:**163–167.
50. **Sivaramakrishnan V, Bidula S, Campwala H, Katikaneni D, Fountain SJ.** 2012. Constitutive lysosome exocytosis releases ATP and engages P2Y receptors in human monocytes. J. Cell Sci. **125:**4567–4575.
51. **Verderio C, Cagnoli C, Bergami M, Francolini M, Schenk U, Colombo A, Riganti L, Frassoni C, Zuccaro E, Danglot L, Wilhelm C, Galli T, Canossa M, Matteoli M.** 2012. TI-VAMP/VAMP7 is the SNARE of secretory lysosomes contributing to ATP secretion from astrocytes. Biol. Cell **104:**213–228.
52. **Nimmerjahn A, Kirchhoff F, Helmchen F.** 2005. Resting microglial cells are highly dynamic surveillants of brain parenchyma in vivo. Science **308:**1314–1318.
53. **Perry VH, O'Connor V.** 2010. The role of microglia in synaptic stripping and synaptic degeneration: a revised perspective. ASN Neuro **2:**e00047. doi:10.1042/AN2010024.
54. **Tremblay ME, Lowery RL, Majewska AK.** 2010. Microglial interactions with synapses are modulated by visual experience. PLoS Biol. **8**(11): e1000527. doi:10.1371/journal.pbio.1000527.
55. **Tremblay ME, Stevens B, Sierra A, Wake H, Bessis A, Nimmerjahn A.** 2011. The role of microglia in the healthy brain. J. Neurosci. **31:**16064–16069.
56. **Wake H, Moorhouse AJ, Jinno S, Kohsaka S, Nabekura J.** 2009. Resting microglia directly monitor the functional state of synapses in vivo and determine the fate of ischemic terminals. J. Neurosci. **29:**3974–3980.
57. **Cirrito JR, Yamada KA, Finn MB, Sloviter RS, Bales KR, May PC, Schoepp DD, Paul SM, Mennerick S, Holtzman DM.** 2005. Synaptic activity regulates interstitial fluid amyloid-beta levels in vivo. Neuron **48:**913–922.
58. **Palop JJ, Mucke L.** 2010. Amyloid-beta-induced neuronal dysfunction in Alzheimer's disease: from synapses toward neural networks. Nat. Neurosci. **13:**812–818.